External cavity diode laser based upon an FBG in an integrated optical fiber platform

Stephen G. Lynch,* Christopher Holmes, Sam A. Berry, James C. Gates, Alexander Jantzen, Teresa I. Ferreiro, and Peter G. R. Smith

Optoelectronics Research Centre, University of Southampton, Southampton, SO17 1BJ, UK

**gl@soton.ac.uk*

Abstract: An external cavity diode laser is demonstrated using a Bragg grating written into a novel integrated optical fiber platform as the external cavity. The cavity is fabricated using flame-hydrolysis deposition to bond a photosensitive fiber to a silica-on-silicon wafer, and a grating written using direct UV-writing. The laser operates on a single mode at the acetylene P13 line (1532.83 nm) with 9 mW output power. The noise properties of the laser are characterized demonstrating low linewidth operation (< 14 kHz) and superior relative intensity noise characteristics when compared to a commercial tunable external cavity diode laser.

OCIS codes: (140.3570) Lasers, single-mode; (230.1480) Bragg reflectors; (130.0130) Integrated optics; (060.3735) Fiber Bragg gratings; (300.6260) Spectroscopy, diode lasers.

References and links

1. K. Petermann, "External optical feedback phenomena in semiconductor lasers," Advanced Networks and Services **1**, 480–489 (1995).
2. R. F. Kazarinov and C. H. Henry, "The relation of line narrowing and chirp reduction resulting from the coupling of a semiconductor laser to passive resonator," IEEE J. Quantum Electron. **23**(9), 1401–1409 (1987).
3. C. J. Hawthorn, K. P. Weber, and R. E. Scholten, "Littrow configuration tunable external cavity diode laser with fixed direction output beam," Rev. Sci. Instrum. **72**(12), 4477 (2001).
4. K. Liu and M. G. Littman, "Novel geometry for single-mode scanning of tunable lasers," Opt. Lett. **6**(3), 117–118 (1981).
5. M. Buric, J. Falk, K. P. Chen, L. Cashdollar, and A. Elyamani, "Piezo-electric tunable fiber Bragg grating diode laser for chemical sensing using wavelength modulation spectroscopy," Opt. Express **14**(6), 2178–2183 (2006).
6. C. A. Park, C. J. Rowe, J. Buus, D. C. J. Reid, A. Carter, and I. Bennion "Single-mode behaviour of a multimode 1.55 μm laser with a fibre grating external cavity," Electron. Lett. **22**(21), 1132–1134 (1986).
7. S. Huang, H. Zhao, and L. Xue, "Frequency stabilization of FBG external cavity laser diode," in Asia-Pacific Conference on Circuits and Systems (IEEE, 2002), pp. 565–567.
8. Y. Sidorin and D. Howe, "Laser-diode wavelength tuning based on butt coupling into an optical fiber," Opt. Lett. **22**(21), 802–804 (1997).
9. E. Luvsandamdin, K. Christian, M. Schiemangk, A. Sahm, A. Wicht, A. Peters, G. Erbert, and G. Tränkle, "Micro-integrated extended cavity diode lasers for precision potassium spectroscopy in space," Opt. Express **22**(7), 7790–7798 (2014).
10. K. Numata, M. Alalusi, L. Stolpner, G. Margaritis, J. Camp, and M. Krainak, "Characteristics of the single-longitudinal-mode planar-waveguide external cavity diode laser at 1064 nm," Opt. Lett. **39**(7), 2101–2104 (2014).
11. K. Numata, J. Camp, M. A. Krainak, and L. Stolpner, "Performance of planar-waveguide external cavity laser for precision measurements," Opt. Express **18**(22), 22781–22788 (2010).

#257070 Received 22 Jan 2016; revised 3 Mar 2016; accepted 7 Mar 2016; published 8 Apr 2016

12. S. Rauch, J. Sacher, "Compact Bragg grating stabilized ridge waveguide laser module with a power of 380 mW at 780 nm," IEEE Photonics Technol. Lett. **27**(16), 1737–1740 (1739).
13. C. Sima, J. C. Gates, and H. L. Rogers, P. L. Mennea, C. Holmes, M. N. Zervas, and P. G. R. Smith, "Ultra-wide detuning planar Bragg grating fabrication technique based on direct UV grating writing with electro-optic phase modulation," Opt. Express **21**(13), 15747–15754 (2013).
14. C. Holmes, J. C. Gates, L. G. Carpenter, H. L. Rogers, R. M. Parker, P. A. Cooper, S. Chaotan, F. R. Mahamd Adikan, C. B. E. Gawith, and P. G. R. Smith, "Direct UV-written planar Bragg grating sensors," Meas. Sci. Technol. **26**(11), 112001 (2015).
15. C. Holmes, J. C. Gates, and P. G. R. Smith, "Planarised optical fiber composite using flame hydrolysis deposition demonstrating an integrated FBG anemometer," Opt. Express **22**(26), 32150–32157 (2014).
16. J. Martin and F. Ouellette, "Novel writing technique of long and highly reflective in-fibre gratings," Electron. Lett. **30**(10), 811–812 (1994).
17. K. O. Hill, B. Malo, F. Bilodeau, D. C. Johnson, and J. Albert, "Bragg gratings fabricated in monomode photosensitive optical fiber by UV exposure through a phase mask," Appl. Phys. Lett. **62**(10), 1035–1037 (1993).
18. L. G. Carpenter, H. L. Rogers, P. A. Cooper, C. Holmes, J. C. Gates, and P. G. R. Smith, "Low optical-loss facet preparation for silica-on-silicon photonics using the ductile dicing regime," J. Phys. D: Appl. Phys. **46**(47), 475103 (2013).
19. Wavelength References, "C-band wavelength calibrator acetylene gas cell $^{12}C_2H_2$" http://www.wavelengthreferences.com/pdf/Data%20C2H2.pdf.
20. S. Camatel and V. Ferrero, "Narrow linewidth CW laser phase noise characterization methods for coherent transmission system applications," J. Lightwave Technol. **26**(17), 3048–3055 (2008).
21. Keysight Technologies, "81480B, 81680/40/72B, 81482B, & 81642B tunable laser modules users guide" http://www.keysight.com/upload/cmc_upload/All/b_tlsB0402.pdf.
22. Redfern Integrated Optics, "RIO PLANEX^{TM} external cavity laser" http://www.rio-inc.com/pdf/Rio_Orion_Planex_Product%20Brief_1.24.14.pdf.

1. Introduction

Diffraction and Bragg gratings can be used in an external cavity diode laser (ECDL) to ensure single mode operation, reduced linewidths [1, 2] and excellent stability. Diffraction grating structures are regularly used to isolate a single longitudinal mode, thereby ensuring single mode operation at the desired wavelength. The most commonly used and commercially available grating-based external cavities are of Littrow [3] or Littman-Metcalf [4] configurations. These configurations have very large tuning ranges, often able to span the entire gain region of the semiconductor gain device. The bulk mechanical nature of these designs can lead to long-term instabilities as the alignment of the laser is vulnerable to both thermal drift and acoustic vibrations. If designed and aligned correctly these systems are capable of tuning over large regions without mode hopping. Other external cavity systems include fiber Bragg-grating cavities [5–8], and volumetric gratings [9].

More recently, Bragg-grating external cavities using glass materials have been to make single mode lasers; these have been made commercially available from Redfern Integrated Optics using a planar platform [10, 11] and Sacher-Laser using a volume holographic grating [12]; such lasers have demonstrated excellent linewidth, low relative intensity noise (RIN) and high side-mode suppression-ratio (SMSR). The planar gratings used are typically made from glasses that have intrinsically low nonlinearity and low losses resulting in higher Q-factor cavities. Glass waveguides can also be fabricated using direct UV-writing techniques that are capable of writing high quality apodized Bragg gratings [13, 14]. Typically these planar waveguides use a silicon substrate, with the advantage that this substrate acts to thermally equilibriate the structure.

We previously demonstrated integration of fiber onto a silicon substrate as a hot-wire anemometer [15]. The integrated optical fiber was fused to a silicon substrate using a flame-hydrolysis deposition (FHD) process that would normally be used in the fabrication of planar waveguides. The fiber is bonded with a mechanically strong and high optical quality glass providing good acoustical and thermal coupling with the silicon substrate, though in this in-

#257070 Received 22 Jan 2016; revised 3 Mar 2016; accepted 7 Mar 2016; published 8 Apr 2016

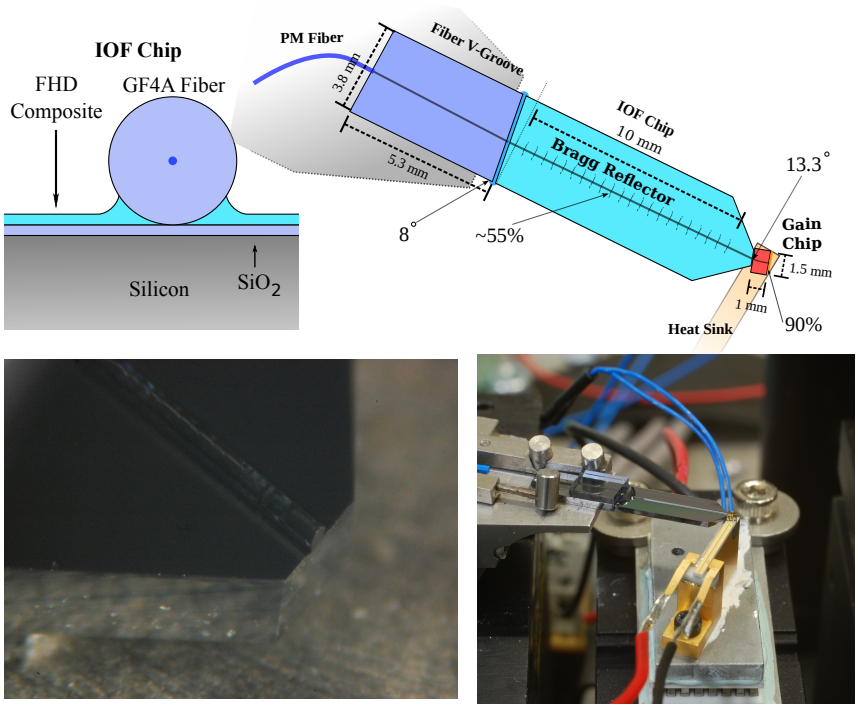

Fig. 1. (Top Left) Cross section of IOF chip. (Top Right) Schematic of ECDL with IOF (Bottom Left) Photograph of external cavity taken through a microscope. The tip of the IOF chip is diced to triangular shape to facilitate alignment with the gain-chip. Reflections along the length of the fiber are chipping of the FHD glass - the fiber remains fully intact. (Bottom Right) Photograph of prototype system.

stance the optical qualities of the bonding material are not exploited, but rather the mechanical strength. The platform has advantages from both fiber and planar technologies where fiber technology is highly developed, providing superior photosensitivity, lower losses and greater complexity and precision in the waveguide structure.

In this Paper we will present an integrated optical fiber (IOF) based ECDL. A photosensitive fiber is fused to a silicon substrate using the technique described in [15], a Bragg grating is then written into the fiber using a direct UV-writing process; the device is diced into a suitable geometry and butt-coupled to a semiconductor gain-chip to form the laser cavity. Section 2 will describe the design considerations and fabrication of the external cavity, detailing the FHD, UV-writing and dicing processes. Section 3 will cover the characterization of the device: the basic laser properties are characterized, demonstrating scanning of P13 acetylene line, and we report some of the radio frequency (RF) properties of the laser including the phase noise and the RIN.

2. Fabrication

The system comprises of a UV-written grating in an IOF chip butt-coupled to an InP gain-chip (Model SAF1126H with 90% reflectivity end facet from Thorlabs Inc). The high thermal conductivity of the silicon substrate helps to heatsink and thermalize the device. The device geometry is precisely designed with angled facets to terminate the ends of the IOF, eliminating unwanted optical feedback, and is arranged to minimize angular-coupling losses between waveguides (see Fig. 1.)

#257070
Received 22 Jan 2016; revised 3 Mar 2016; accepted 7 Mar 2016; published 8 Apr 2016

2.1. *Integrated optical fiber fabrication*

The optical fiber is integrated onto the surface of a silicon wafer using a consolidated glass composite. This integration of the fiber provides a thermally stable and mechanically fixed platform for device fabrication. Established fiber drawing technology allows for intricate and precise fiber geometries to be fabricated with low loss waveguides; much lower than would be achievable in standard planar glass waveguides. Waveguide losses are usually measured in units of dB/cm; given we are starting in low loss fiber we are unable to measure any significant loss over short lengths.

For this research the fiber used was GF4A (Sold by Thorlabs Inc). This fiber has a small 4.0 μm mode-field diameter (MFD) and is doped with germanium and boron to make the fiber photosensitive to direct UV-writing. This is well matched to the vertical MFD of the gain-chip reducing loss associated with butt-coupling to the waveguide. The gain-chip near-field is considered to be Gaussian to estimate the coupling loss, the near-field coupling loss would result in a modeled loss of 1.2 dB by using GF4A fiber compared with a 6.8 dB loss if SMF-28 fiber were used in the IOF.

The FHD process that would normally be used to produce planar waveguides is used to bond the fibers. The fibers are carefully laid over the surface of a polished silicon wafer with a 1.3 μm thick layer of thermally grown silicon dioxide. In the FHD process gaseous precursors pass through a hydrogen-oxygen flame and deposit an oxide "soot" onto the surface of the wafer and fiber. This soot is then consolidated in a furnace above 1000 °C forming a glass layer. This results in a mechanically strong glass meniscus that bonds the underside of the fiber directly on the surface of the wafer as seen in Fig. 1.

2.2. *UV-writing*

High intensity UV light can be used to induce refractive index changes in photosensitive glasses. This mechanism has been exploited to write Bragg gratings and waveguides in fibers, and also planar waveguides in a process known as UV-writing. There are various methods for writing gratings in fibers, one of the most widely used for fiber Bragg grating (FBG) production is the phase-mask technique [16, 17]. The system used in this work is a direct UV-writing process that writes Bragg gratings. The technique uses a 244 nm laser split into two coherent beams, these beams are focused to the same point in the core of the fiber forming interference fringes. The angle between the two beams determines the fringe periodicity; these fringes determine the periodicity of the Bragg grating, though the small spot size permits detuning over a wide range of Bragg wavelengths (1200 nm to 1900 nm) [13]. Precision air-bearing stages translate the IOF chip along the length of the fiber, the interference fringes are shifted simultaneously in line with the IOF chip by controlling the phase delay of one UV beam using an electro-optic modulator (EOM). Control of the phase allows us to software control the apodization function and the detuning of the grating.

The fiber dispersion of this device was carefully characterized so that the grating was written precisely overlapping an acetylene line; for this research it was written at the P13 line (1532.83 nm). The grating is uniform and 10 mm long, providing a reasonably narrow line grating. The grating reflectivity was measured to be $\sim 55\,\%$; by cleaving the end facet of the chip, the reflected light at the grating resonance is compared against the detuned reflected light of the end facet whose index and reflectivity is known (3.4 %). The spectral response of the grating was measured on an optical spectrum analyzer (OSA) using an amplified spontaneous-emission source and can be seen in Fig. 2, the grating has a −3 dB bandwidth of 18 pm.

#257070 Received 22 Jan 2016; revised 3 Mar 2016; accepted 7 Mar 2016; published 8 Apr 2016

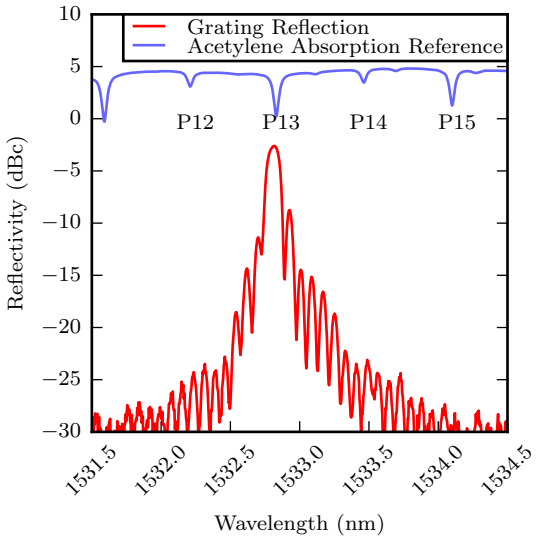

Fig. 2. Grating reflection spectrum for an unapodized grating used in the laser external cavity with −3 dB bandwidth of 18 pm. The acetylene absorption spectrum has been overlaid for comparison with lines of the P-branch labeled and uses the same log scaling but arbitrary offset. The acetylene spectrum shown was obtained from the internal acetylene cell in the OSA used for calibration.

2.3. Dicing and polishing

The IOF external cavity needed two angled facets to be machined: one to minimize angular coupling loss into the gain-chip and one to match the angled pigtailed that would then be adhered to the external cavity. The angled facets were prepared using a commercial semiconductor dicing machine. For the purpose of facet preparation the blade choice and dicing parameters are optimized to dice silica and other glass composites in the ductile dicing regime, offering low roughness waveguide end facets [18]. This technique can be used as an alternative to polishing and is a simpler and faster method - the entire chip can be shaped and polished in one process step.

A sufficiently large angle is needed at the interface between the planar glass waveguide and the InP gain-chip waveguide to suppress reflections, preventing a parasitic internal cavity from being formed; the gain-chip's waveguide is designed with an angled exit to the facet for this reason. For optimal butt-coupling to the InP gain-chip, the external cavity has an angled facet at 13.3° to the normal of the waveguide. This angle was computed simply from Snell's law with knowledge of the effective index of the IOF and the output angle of the gain-chip into air. To couple light out of the laser cavity a pigtail held in a V-groove assembly is butt-coupled to the end of the planar chip. The fiber pigtail is a standard telecommunications PM-fiber held in a V-groove assembly that is polished at 8° for low return loss. To accommodate this angle the planar chip was also diced on the pigtail end at 8° as the chips have similar effective indices. The V-groove pigtail is permanently bonded in place by using a refractive index matched, UV-curing, optical adhesive.

3. Characterization

The IOF external cavity is bonded to a V-groove assembly that acts to couple out the laser radiation. This V-groove assembly is clamped to a mount attached to a multi-axis stage system. The gain-chip is bonded to a heatsink that rests on a thermoelectric-cooler (TEC). The stage

#257070 Received 22 Jan 2016; revised 3 Mar 2016; accepted 7 Mar 2016; published 8 Apr 2016

system is used to align the IOF to the gain-chip waveguide. The pigtail emerging from the V-groove assembly couples out the laser radiation and is connected to a 60 dB fiber isolator. The stage systems are mounted on a breadboard that is isolated to reduce susceptibility to room vibrations. The experimental setup can be seen in Fig 1, the angled cuts of the components can be seen; note there is a small air gap between the gain-chip and the IOF chip and they are not directly bonded.

The free spectral range (FSR) of the cavity is ~ 7.5 GHz (59 pm) corresponding to an effective optical cavity length of 20 mm; this value was directly measured from the OSA and corresponds to the actual cavity length, the group indices of the IOF and gain chip, and the phase response of the strong Bragg grating. The grating reflector is sufficiently narrow to ensure only one longitudinal mode can lase. The laser power characteristic with injection current is shown in Fig. 3. with a threshold at 50 mA. A consequence of a narrow grating spectrum compared to the FSR is that a mode hops causes significant changes in the output power of the laser as seen by the large discontinuity in Fig. 3, this is an unintended consequence of using such a long unapodized grating. This mode hop occurs as the laser mode moves to a regime where the feedback provided by the grating is smaller. The laser then hops to operate on a different active mode where there is greater feedback, but consequently lower output coupling, causing the drop in output power. This could be mitigated by apodizing the profile or chirping the grating period to broaden its spectral response and obtain a more linear power curve. This results in the nonlinear relationship between current and output power, as the current is increased the active longitudinal mode sweeps across the bandwidth of the grating and the grating reflectivity is highly wavelength dependent, changing the overall cavity Q-factor. In this setup avoidance of mode hopping could be achieved by adjusting the cavity length using the translation stages, enabling tuning of the small air gap between the IOF and gain-chip. The grating provides suppression of unwanted modes with an SMSR of > 60 dB (see Fig. 3.) and decreasing to ~ 45 dB on the verge of mode hopping. Note that the spectral shape, including the shoulder seen in Fig. 3, is an artifact of the OSA and not a feature of the lineshape of the laser spectrum.

To determine the absolute frequency and tuning capability the laser was tuned over an acetylene line by modulating the injection current of the laser with a triangle wave. The laser output is split, one half of the signal is passed through the acetylene cell [19] and the ratio of the filtered and unfiltered light is measured. The resulting gas line scan can be seen in Fig. 4.

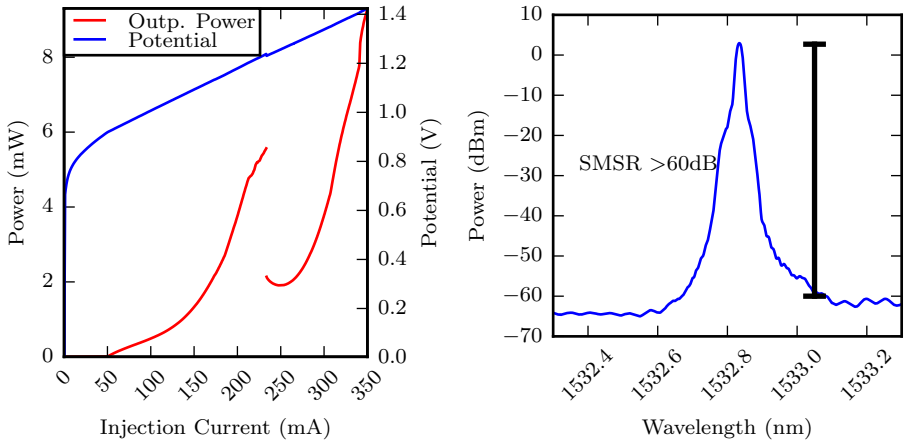

Fig. 3. (Left) Power current curve of laser. Threshold was measured at 50 mA. A mode hop occurs at 233 mA. (Right) Spectrum of laser taken on OSA with 20 pm resolution bandwidth. The spectrum indicates a ~ 60 dB SMSR.

#257070 Received 22 Jan 2016; revised 3 Mar 2016; accepted 7 Mar 2016; published 8 Apr 2016

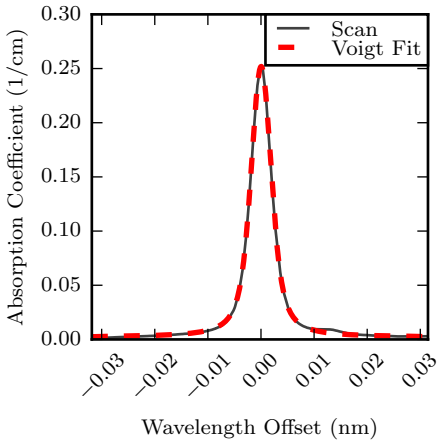

Fig. 4. Scan of the P13 Acetylene line. Acetylene gas cell is held at a pressure of 20 Torr (2.67 kPa).

The laser signal was measured using a 16 GHz photodiode, the resulting signal provides intensity noise information. Measuring the RF noise characteristics directly using a photodiode signal provides information on the RIN (Fig. 5). As the existing prototype arrangement is mounted on translation stages there is significant instability nearer the low frequencies due to increased susceptibility to acoustics and thermal drifts; it is expected that if the external cavity and gain-chip were bonded to a monolithic substrate this would significantly reduce the effects of the thermal fluctuations and susceptibility to acoustical effects. At higher frequencies the noise floor is limited to around -150 dBc/Hz which is the shot noise limit at the measured optical power.

To accurately measure the frequency noise or linewidth property of the laser a heterodyne technique with another narrow linewidth laser is used. The resulting beat note is recorded on a 3 GHz bandwidth oscilloscope and multiple time traces are taken. The data is Hilbert transformed, the complex phase information is singled out, and the power spectral density (PSD) is computed using Welch's method with a Hanning window, and then further averaged for each trace. Obtaining the phase noise gives a more complete description of the noise instabilities; instabilities of the intrinsic Lorentzian linewidth are not overestimated due to fluctuations in the line that would be typically obtained by using a delayed self-heterodyne measurement and measuring the linewidth on a RF spectrum analyzer, this is explained in detail in [20].

The laser signal of the IOF was mixed with the signal from an Agilent 81640B on a photodiode and the beat signal recorded by digital sampling on an oscilloscope. The time signal was post processed to produce a phase noise plot. Using the phase noise model specified by Camatel and Ferrero [20], and fitting it to the phase noise the Lorentzian linewidth is measured to be 14.2 kHz. Although the Agilent tunable laser is specified at 100 kHz [21], which was determined using a delayed self-heterodyne measurement, Camatel and Ferrero measured the Lorentzian linewidth of a similar Agilent laser to be only 8 kHz [20] with the same specification. Their measurement was obtained using an optical phase locked loop (OPLL) and a Michelson interferometer method and then fitting the same noise model as used in our phase noise plots. A similar laser system Given that the width of the Lorentzian spectrum obtained from a beat-note signal is the sum of both laser Lorentzian widths we can at least specify that the IOF laser has a linewidth of < 14 kHz. To put this into context commercial RIO planar lasers have Lorentzian linewidths as low as ≤ 2 kHz [22] and the Sacher-Laser volume holographic grating laser has a linewidth of 18 kHz [12].

#257070 Received 22 Jan 2016; revised 3 Mar 2016; accepted 7 Mar 2016; published 8 Apr 2016

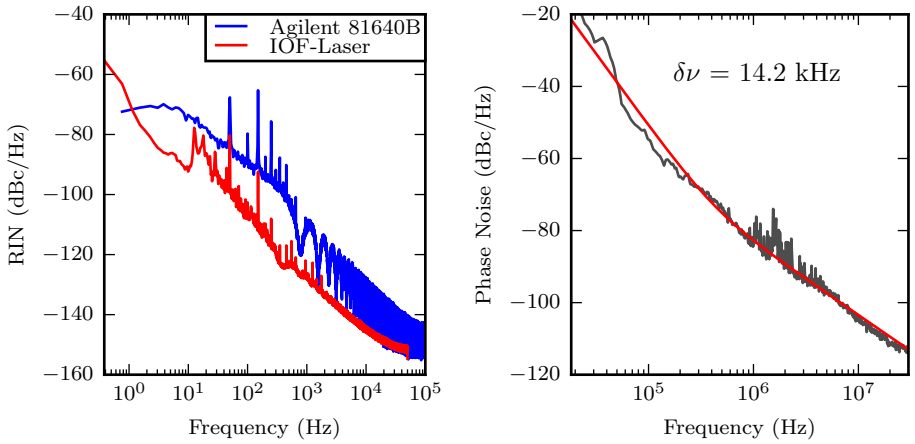

Fig. 5. (Left) RIN of the the IOF laser measured for 10 s compared with a tunable Agilent 81640B measured for 1 s. Peaks can be seen at 50 Hz and its harmonics. Much of the low frequency noise is dominated by acoustics. The current prototype setup is susceptible to vibrations and thermal fluctuations in the environment. This measurement was taken at 1532.86 nm, with an injection current of 320 mA, and the optical power attenuated down to ~ 0.5 mW. (Right) The phase noise plot derived from the beat note of the an Agilent 81640B laser and the IOF laser measured for 5 ms. The plot is fitted to noise parameters as specified by [20]. The Lorentzian linewidth is given as 14.2 kHz - this linewidth is the sum of linewidths of the Agilent and IOF lasers. This measurement was taken at 1532.86 nm, with an injection current of 320 mA and an optical power of 5 mW.

4. Conclusion

We have demonstrated the suitability of UV-written Bragg gratings on a novel IOF platform as the external cavity. The IOF platform allows us to utilize a low loss, photosensitive fiber, with a small MFD, improving the mode matching with the gain-chip whilst retaining the stability advantages of being planarized. The system is extremely compact and the fabrication process steps are repeatable, relatively simple and scale well to batch production. We show precise grating writing as demonstrated by targeting the Bragg wavelength to the acetylene P13 line. The laser shows low intensity noise compared with a commercial bulk laser, and low phase noise characteristics comparable to other state-of-the-art long-cavity external cavity lasers. This demonstrates the suitability of this source for high resolution spectroscopy and coherent sensing.

Acknowledgments

This work is supported by the UK EPSRC grants EP/I003835/1 and EP/K503150/1. Data associated with this publication can be accessed via URL http://dx.doi.org/10.5258/SOTON/384728.

#257070 Received 22 Jan 2016; revised 3 Mar 2016; accepted 7 Mar 2016; published 8 Apr 2016